

Surface Plasmon Resonance Imaging Analysis of Protein-Receptor Binding in Supported Membrane Arrays on Gold Substrates with Calcinated Silicate Films

K. Scott Phillips, Thomas Wilkop, Jiing-Jong Wu, Rabih O. Al-Kaysi, and Quan Cheng*

Department of Chemistry, University of California, Riverside, California 92521

Received April 21, 2006; E-mail: quan.cheng@ucr.edu

Surface plasmon resonance imaging (SPRi) is a powerful tool for label-free and real-time studies of biological interactions,^{1–4} with the potential for high-throughput analysis in crucial areas such as pharmaceutical screening and proteomics. The surface functionalization chemistry for gold SPR substrates is primarily based on alkanethiol SAMs, and involves soft lithography,¹ spotting,^{2,3} microcontact printing,⁴ and microfluidic patterning.⁵ In addition to protein and DNA analysis, SPR has also been a key method for studies of cell membrane components.⁶ However, the development of robust and fluid lipid membrane arrays on gold surfaces is a major challenge that has been met with limited success.⁷ Glass surfaces, on the other hand, have been extensively studied for fabrication of membrane patches and arrays. Several groups have made great strides in the development of supported bilayer membrane (SBM) arrays on glass^{8,9} and for GPCRs,¹⁰ which can be used for high-throughput screening studies. We recently demonstrated that thin (5–50 nm) glassy layers can be produced on gold substrates using layer-by-layer assembly and calcination.¹¹ The nanoscale silicate coatings are stable for days in buffer, allow for SPR spectroscopic analysis with high sensitivity, and exhibit reduced nonspecific adsorption.¹¹

Given that most efforts to characterize membrane arrays and their interactions have relied on fluorescence techniques, combining SPRi with these arrays would offer a new tool to monitor binding in real-time and investigate affinity properties without the need of labels. Here we report the fabrication of three-dimensional features on calcinated surfaces to generate membrane arrays for SPR imaging studies. The method takes advantage of desirable properties of glass that allow for its facile manipulation. To pattern the substrates with “nanowell” arrays for SPR imaging, a standard photolithographic process was utilized (Scheme 1). Shipley 1813 photoresist was spun onto the calcinated films at 3500 rpm, and both TEM grids and homemade photomasks were used for the UV exposure step, followed by controlled etching with HF.

Scheme 1. Fabrication Sequence for the Creation of Nanowells.

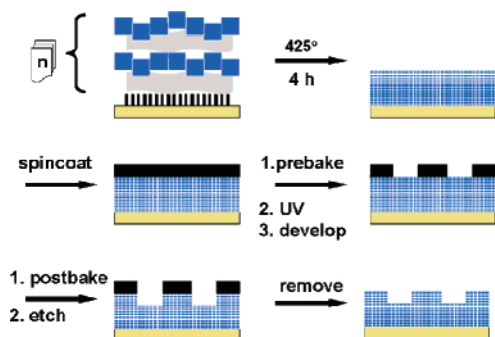


Figure 1 shows SPR and AFM images of patterned substrates. The top image is from two four-well arrays imaged in air. Visual

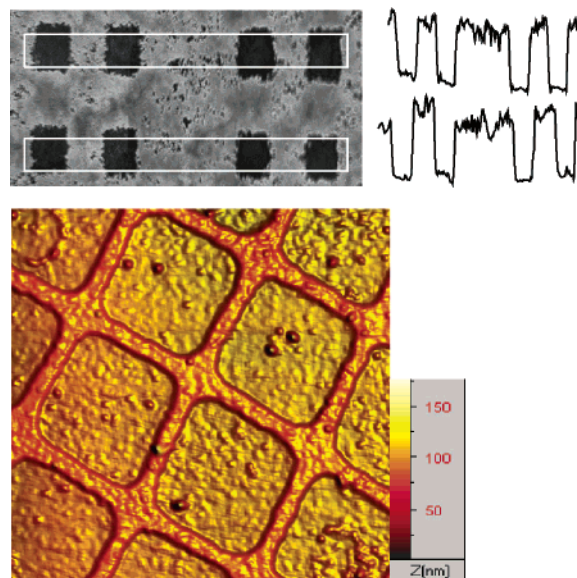


Figure 1. Top: SPR image and reflectivity profile of an array of $200 \times 200 \mu\text{m}$ wells. Bottom: AFM image of 30-layer calcinated film etched with 0.1 M HF. A 1000-mesh TEM grid was used as the photomask.

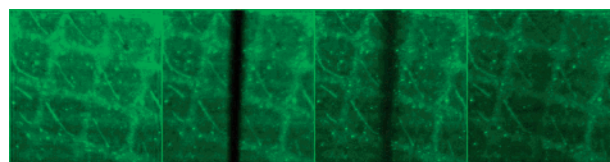


Figure 2. FRAP results for the membranes on the etched surface. From left to right: before bleaching, 5 s, 35 s, and 10.75 min after bleaching.

inspection of a reflectivity profile averaged across the wells (top right) shows excellent reproducibility. The bottoms of the wells have less deviation than the top surface, indicating that the etching has a smoothing effect. This was verified by AFM analysis of patterns on calcinated films made with TEM grids as photomasks. The $25 \times 25 \mu\text{m}$ squares were reproduced with fidelity in the silicate material, and a $2.1 \pm 0.6 \text{ nm}$ RMS roughness ($n = 4$) was obtained within the nanowells. Some defect features were found on the nanometer scale, as previously observed with SEM.¹⁰ The well depth was controlled by etching time and HF concentration, resulting here in 18 nm wells for a film etched for 60 s with 0.1 M HF.

To demonstrate the capacity of the glassified nanowell array substrates to support fluid bilayer membranes, fluorescence recovery after photobleaching (FRAP) experiments were performed on etched surfaces. Figure 2 shows a series of FRAP images for 2% NBD-PC doped SBMs on a TEM grid patterned substrate. The wells exhibit less fluorescence intensity because they are closer to the

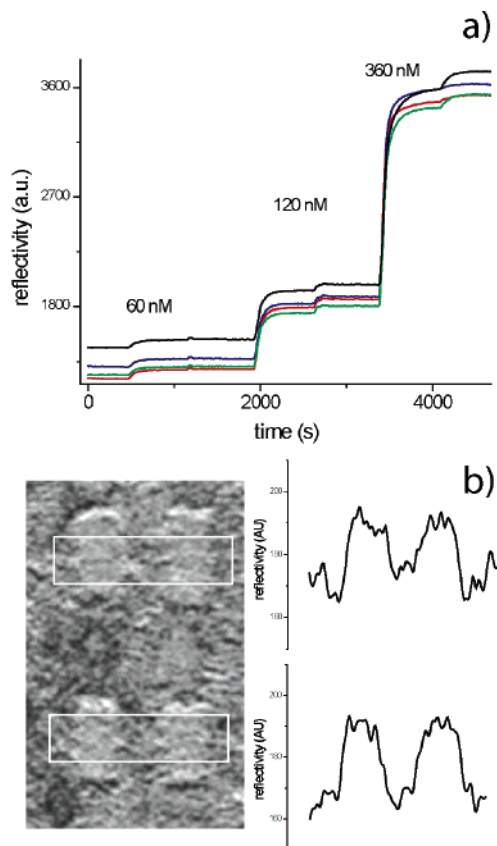


Figure 3. (a) SPR sensorgrams for the binding of different concentrations of CT in nanowells and (b) SPR difference image and profile for binding of 12 nM CT to GM1-containing membranes in nanowells.

gold substrate and experience a higher degree of quenching by nonradiative energy transfer. Bleach lines recovered completely and showed a lateral diffusion value of $1.1 \pm 0.5 \mu\text{m}^2/\text{s}$ ($n = 10$), similar to that for glass and PDMS,¹² indicating that the membranes are fluid. Lateral mobility of this magnitude is considered evidence of a true “bilayer membrane” rather than immobile “hybrid membranes” and is crucial for biomimicry because many membrane-associated interactions depend on free rearrangement of receptor molecules in membranes. This could also affect the accuracy of measurement with SPRi, because many interactions are strengthened by multivalency, in which the first binding interaction restricts the ligand within range of the second binding site, decreasing the entropic barrier for further events.¹³ Without fluidity, ligands with multiple subunits may not bind to SBM-supported receptors through a mechanism similar to that in a real cell membrane.

We further tracked the fusion of egg PC vesicles and followed binding events in the nanowells. The vesicles were first injected and incubated for 1 h, followed by rinsing with buffer. The shape of the curve associated with fusion inside the wells (Supporting Information) is similar to that previously found on calcinated substrates.¹¹ To explore the analysis of specific ligand–receptor interactions in an array fashion, vesicles were doped with 5 mol % ganglioside GM1 and fused on the substrates. Cholera toxin (CT), a bacterial toxin with five B subunits that bind to GM1 before insertion into the cell membrane, was injected over the substrate through a flow cell. Figure 3a shows the SPRi sensorgrams for

several concentrations of CT in four nanowells. Control experiments (SI) revealed no detectable signal change for the nonspecific adsorption of 600 nM CT to PC membranes without GM1. The measured reflectivity between wells is highly reproducible, with only 8% RSD for 60 nM CT. This is significant because the duplication of binding results obtained in different wells is essential in large-scale screening applications. Figure 3b is the SPRi difference image obtained by subtracting an image before injection of toxin from that after injection, demonstrating that concentrations as low as 12 nM could easily be distinguished in the wells without any blocking on the top surface. We attribute the increased signal in the wells to the different decay length of the evanescent field in the direction normal to the gold surface. Because vesicle fusion and toxin binding occur both inside and outside of the wells, the difference in response is a result of the higher field strength in the wells, which are closer to the gold. Remarkably, the sensitivity with nanowell substrates is higher than that achieved with a spectroscopic SPR system¹¹ and appears to be better than values reported for the detection of protein toxins with SAM-based methods.¹⁴ Therefore, loss of signal due to the nanoscale glassy layer does not seem to constitute a major limitation if the wells are fabricated close enough to the gold surface.

In conclusion, we have demonstrated a novel method to generate silicate nanowells on gold substrates for SPR imaging analysis of toxin–receptor interactions in membrane arrays. The method allows for nonlabeled detection with high sensitivity and has great potential for high-throughput analysis of ligand/receptor or protein/protein interactions that require a fluid membrane environment. Implementation of membrane arrays with individual addressability is currently under investigation.

Acknowledgment. The authors thank Dr. Chris Bardeen for AFM use and Dr. Pingyun Feng and Xiqing Wang for the help with calculation. The work is supported in part by a grant (BES-0428908) from NSF.

Supporting Information Available: Control experiments, vesicle fusion curve in nanowells, detailed procedures for vesicle preparation, fabrication of nanowell substrates, and AFM analysis. This material is available free of charge via the Internet at <http://pubs.acs.org>.

References

- (1) Frey, B. L.; Jordan, C. E.; Kornuth, S.; Corn, R. M. *Anal. Chem.* **1995**, *67*, 4452–4457.
- (2) Shumaker-Parry, J. S.; Aebersold, R.; Campbell, C. T. *Anal. Chem.* **2004**, *76*, 2071–2082.
- (3) Wolf, L. K.; Fullenkamp, D. E.; Georgiadis, R. M. *J. Am. Chem. Soc.* **2005**, *127*, 17453–17459.
- (4) Wilkop, T.; Wang, Z.; Cheng, Q. *Langmuir* **2004**, *20*, 11141–11148.
- (5) Smith, E. A.; Thomas, W. D.; Kiessling, L. L.; Corn, R. M. *J. Am. Chem. Soc.* **2003**, *125*, 6140–6148.
- (6) Bieri, C.; Ernst, O. P.; Heyse, S.; Hofmann, K. P.; Vogel, H. *Nat. Biotechnol.* **1999**, *17*, 1105–1108.
- (7) Morigaki, K.; Baumgart, T.; Jonas, U.; Offenhausser, A.; Knoll, W. *Langmuir* **2002**, *18*, 4082–4089.
- (8) Groves, J. T.; Boxer, S. G. *Acc. Chem. Res.* **2002**, *35*, 149–157.
- (9) Cremer, P. S.; Yang, T. *J. Am. Chem. Soc.* **1999**, *121*, 8130–8131.
- (10) Fang, Y.; Frutos, A. G.; Lahiri, J. *J. Am. Chem. Soc.* **2002**, *124*, 2394–2395.
- (11) Phillips, K. S.; Han, J.-H.; Martinez, M.; Wang, Z.; Carter, D.; Cheng, Q. *Anal. Chem.* **2006**, *78*, 596–603.
- (12) Phillips, K. S.; Cheng, Q. *Anal. Chem.* **2005**, *77*, 327–334.
- (13) Crothers, D. M.; Metzger, H. *Immunochemistry* **1972**, *9*, 341–357.
- (14) Choi, K.; Seo, W.; Cha, S.; Choi, J. *J. Biochem. Mol. Biol.* **1998**, *31*, 101–105.

JA0628102